Alkane Contamination Effects on PFPE Lubricant Bonding to a-CH_x Overcoats

Ryan Z. Lei and Andrew J. Gellman*

Department of Chemical Engineering, Carnegie Mellon University, Pittsburgh, Pennsylvania 15213

Christopher F. McFadden

Advanced Development Laboratories, Quantum Corporation, Shrewsbury, Massachusetts 01545

Received March 19, 2001. In Final Form: July 19, 2001

Increasing operating temperatures within hard disk drives promote increased outgassing from drive components and thus can adversely influence the durability and reliability of hard disk drives. This study investigates the effects of hydrocarbon contamination on the bonding of perfluoropolyalkyl ether (PFPE) lubricants to amorphous hydrogenated carbon (a-CH_x) overcoats. This work has used decane ($C_{10}H_{22}$) as a model for the hydrocarbon contamination present in drives and perfluorodiethyl ether ($(CF_3CF_2)_2O$) and 2,2,2-trifluoroethanol (CF_3CH_2OH) as models for the backbone and endgroups, respectively, of the common disk lubricant Fomblin Zdol. Temperature-programmed desorption experiments were conducted using CF_3CH_2OH coadsorbed with $C_{10}H_{22}$ on an a-CH_x overcoat and $(CF_3CF_2)_2O$ coadsorbed with $C_{10}H_{22}$ on an a-CH_x overcoat. The results indicate that the presence of $C_{10}H_{22}$ decreases the adsorption energies of both CF_3CH_2OH and $(CF_3CF_2)_2O$ on the a-CH_x overcoats. The implication of these results is that the mobility of PFPE lubricant films can be increased by the presence of hydrocarbon contaminants on the disk surface.

1. Introduction

Data storage in hard disk drives uses a 150−300 Å layer of magnetic material deposited on a hard disk as the medium for data storage. Data are written to and read from the magnetic film by a small recording head that flies over the surface of the disk as it spins. A 50−100 Å thick hydrogenated or nitrogenated amorphous carbon overcoat (a-CH_x and a-CN_x, respectively) is sputtered onto the magnetic film to protect it from damage due to intermittent contacts between the recording head and disk surface.[1] For additional protection, a 5−20 Å layer of perfluoropolyalkyl ether (PFPE) lubricant is applied to the surface of the amorphous carbon overcoat.[1−3] The recording head flies over the disk surface and lubricant film on a layer of air less than 300 Å thick.[1,4] Since 1991, the areal recording density (the number of bits stored per unit area) has maintained a growth rate of 60% per year.[5] To continue this growth rate, the head−disk spacing must be decreased continuously. Ultimately, there will only be room for a few atomic and molecular layers of overcoat and lubricant to protect the magnetic media from contact with the head. With such small head−disk spacing, a fundamental understanding of the molecular interactions at the head−disk interface is essential for optimizing data protection and thus increasing storage density.

To improve data access times, disks need to be spun at speeds in excess of 10 000 revolutions per minute. As a result of increasing spindle speeds, there has been an increase in operating disk drive temperatures. Higher temperatures within the drive promote increased outgassing from drive components that can influence the tribological properties at the head−disk interface. Smith investigated the atmospheric composition of a typical disk drive during operation by taking air samplings of the drive's interior.[6] Vaporized components from common solvents, products of adhesive and elastomer initiators, adhesive monomers and primers, grease constituents, elastomeric monomers, and plasticizers were found in the drive atmosphere. These chemicals were either constituents of the components used to fabricate the drive or were used in their manufacture. The chemicals were analyzed by a GC/MS and classified as aliphatic and aromatic hydrocarbons, alcohols, ketones, esters, amines, organic acids, and organo-sulfur compounds. Fowler and Geiss performed a similar analysis by placing activated charcoal within an operating disk drive to adsorb chemical vapors.[7] The chemicals captured in this way were found to be predominantly alkane hydrocarbons. Chemical contamination within the operating disk drive is known to cause increased static friction when enough contaminants coalesce to form droplets at the head−disk interface.[8−12]

The goal of our investigation has been to obtain a fundamental understanding of the molecular interactions between contaminants, lubricants, and the a-CH_x overcoats. The industry standard PFPE lubricant is Fomblin

* To whom correspondence should be addressed.

(1) Gellman, A. J. *Curr. Opin. Colloid Interface Sci.* **1998**, *3*, 368−372.
(2) Coffey, K. R.; Raman, V.; Staud, N.; Pocker, D. J. *IEEE Trans. Magn.* **1994**, *30*, 4146−4148.
(3) O'Conner, T. M.; Back, Y. R.; Jhon, M. S.; Min, B. G.; Yoon, D. Y.; Karis, T. E. *J. Appl. Phys.* **1996**, *79*, 5788−5790.
(4) Mate, C. M.; Homola, A. M. In *Micro/Nanotribology and its Applications*; Bhushan, B., Ed.; Kluwer Academic Publishers: The Netherlands, 1997; pp 647−661.
(5) Kryder, M. H. *MRS Bull.* **1996**, *9*, 17−19.
(6) Smith, J. H. *IDEMA Tribology Symposium* **2000**, 79−95.
(7) Fowler, D. E.; Geiss, R. H. *IEEE Trans. Magn.* **2000**, *36*, 133−139.
(8) Gui, J.; Marchon, B. *IEEE Trans. Magn.* **1998**, *34*, 1804−1806.
(9) Gao, C.; Dai, P.; Vu, V. *J. Tribol.* **1999**, *121*, 97−101.
(10) Jesh, M. S.; Segar, P. R. *STLE Tribol. Trans.* **1999**, *42*, 310−316.
(11) Smallen, M. J.; Mee, P. B. *J. Information Storage Processing Systems* **1999**, *1*, 265−271.
(12) Smallen, M. J.; Mee, P. B.; Merchant, K.; Smith, S. *IEEE Trans. Magn.* **1990**, *26*, 2505−2507.

10.1021/la010413t CCC: $20.00
Published on Web 08/31/2001

Zdol [$HO-CH_2CF_2-(OC_2F_4)_n-(OCF_2)_m-OCF_2CH_2-OH$], the structure of which consists of an ether-like backbone with hydroxyl endgroups. To measure the strength of interactions between adsorbates and the hard disk surface, we have used thermally programmed desorption (TPD) spectroscopy. This measurement involves heating a disk surface in a vacuum and using a mass spectrometer to measure the rates of desorption of adsorbed species. Since Fomblin Zdol decomposes when heated on a hard disk surface, it is not possible to obtain molecular TPD spectra of Fomblin Zdol itself.[13,14] Instead, perfluorodiethyl ether ($(CF_3CF_2)_2O$) was used to model its ether-like backbone and 2,2,2-trifluoroethanol (CF_3CH_2OH) was used to model its hydroxyl end groups. To study alkane contamination effects on Fomblin Zdol bonding to a-CH_x films, TPD spectra were obtained of $(CF_3CF_2)_2O$ coadsorbed with decane ($C_{10}H_{22}$) and CF_3CH_2OH coadsorbed with $C_{10}H_{22}$ on a-CH_x films.

The bonding mechanism of fluoroethers and fluoroalcohols to amorphous carbon overcoats has been examined in prior work. Cornaglia and Gellman conducted a study of the bonding of PFPE lubricants to a-CH_x overcoats by using small fluorocarbon ethers and their hydrogenated analogues.[15] They concluded that ethers interact with a-CH_x surfaces through electron donation from the oxygen lone pairs, also known as dative bond bonding. This same model has been proposed for the bonding of ethers to several metal surfaces.[16−21] Paserba et al. investigated the surface chemistry of fluoroethers and fluoroalcohols adsorbed on a-CN_x films and concluded that alcohols interact with the surface through hydrogen bonding.[22]

The focus of the study reported in this paper was to determine the effect of an alkane contaminant on the dative bond of the fluoroethers and the hydrogen bond of the fluoroalcohols to a-CH_x films. We have studied the coadsorption of $C_{10}H_{22}$ with $(CF_3CF_2)_2O$ and the coadsorption of $C_{10}H_{22}$ with CF_3CH_2OH on a-CH_x-coated disks obtained from Quantum Corp. and Seagate Corp. TPD experiments have shown that the desorption energies of both $(CF_3CF_2)_2O$ and CF_3CH_2OH decrease with increasing $C_{10}H_{22}$ coverage on disks provided by both manufacturers. Furthermore, about 0.20 monolayer (ML) of $C_{10}H_{22}$ was enough to displace both $(CF_3CF_2)_2O$ and CF_3CH_2OH into the multilayer adsorption regime. The results of this work suggest that there can be an increase in PFPE lubricant mobility on disk surfaces, even with low levels of alkane contamination.

2. Experimental Section

All experiments were performed in an ultrahigh vacuum (UHV) chamber with a base pressure of $<10^{-10}$ Torr achieved through use of a cryo-pump and a titanium sublimation pump. The chamber is equipped with two leak valves fitted with a stainless steel dosing tube. One of the leak valves is used to introduce vapor of the model lubricants (CF_3CH_2OH or $(CF_3CF_2)_2O$) into the chamber, while the other is used to introduce $C_{10}H_{22}$ vapor into the chamber. The chamber is also equipped with an Ametek Dycor quadrupole mass spectrometer (QMS), which has a mass range of 1−200 amu and is capable of monitoring up to eight masses simultaneously during TPD experiments.

Quantum Corp. and Seagate Corp. supplied magnetic hard disk platters sputter coated with a protective a-CH_x overcoat and no lubricant. The Seagate disks, denoted by a-CH_{Seag}, were sputtered in a 15% H_2 atmosphere. The atmospheric H_2 content for the Quantum disks (a-CH_{Quan}) is unknown. These platters were machine-punched to produce ∼12.5 mm diameter disk samples for use in the UHV chamber. Two tantalum wires were spot-welded to the edge of the sample and mounted to a sample holder at the end of a manipulator. Once mounted to the manipulator, the disk sample could be cooled to ∼100 K through contact with a liquid nitrogen reservoir and heated resistively at a constant rate to the melting point of aluminum. The sample temperature was measured using a chromel−alumel thermocouple spot-welded to the rear face of the sample.

The disk samples were used for the TPD experiments as received. Once inside the chamber, cleaning consisted of simply heating to 400 K to induce desorption of adsorbed species such as water. The TPD spectra obtained during this initial heating did not reveal any desorption. This is not surprising since to achieve UHV conditions the chamber and the sample were subjected to a bakeout in a vacuum for ∼12 h at roughly 400 K. Following this initial treatment, the condition of the surface, as determined by $C_{10}H_{22}$, $(CF_3CF_2)_2O$, and CF_3CH_2OH adsorption and desorption, was highly reproducible. Irreversible changes such as dehydrogenation that do influence adsorbate desorption spectra do not occur until the a-CH_x overcoats are heated to temperatures in excess of 500 K.[15] The primary point is that the sample preparation was sufficient to generate highly reproducible surfaces from the point of the experiments conducted in this work and that, as will be shown, the a-CH_x films provided by Seagate and by Quantum showed very similar effects of alkane contamination on lubricant−surface interactions. Thus, we believe that the results reported in this work are general in nature and not specific to the films produced by either supplier.

The decane [$C_{10}H_{22}$, 99+%] used in this investigation was purchased from Aldrich Chemical Co., Inc. The perfluorodiethyl ether [$(CF_3CF_2)_2O$, 90+%] was purchased from Stem Chemicals, and the 2,2,2-trifluoroethanol [CF_3CH_2OH, 99.5%] was purchased from Lancaster Chemicals. All compounds used were further purified before use through a series of freeze−pump−thaw cycles intended to remove any high vapor pressure contaminants.

Within the UHV chamber, the sample was positioned adjacent to the stainless steel dosing tube and approximately 1 cm from the aperture to the QMS. The procedure for TPD experiments consisted of three steps: adsorption, desorption, and detection. The adsorption step entailed cooling the disk sample to <100 K and exposing its surface to $C_{10}H_{22}$ and then to either the $(CF_3CF_2)_2O$ or the CF_3CH_2OH at pressures between 10^{-9} and 10^{-8} Torr for periods of 30−300 s. The exposures are reported in units of langmuirs (1 langmuir = 10^{-6} Torr s; denoted as L in figures). Experiments were also conducted by adsorbing either $(CF_3CF_2)_2O$ or the CF_3CH_2OH first then $C_{10}H_{22}$ in order to investigate any effects of the order of exposure. Desorption involved heating the sample at a constant rate of 2 K/s from 100 to 400 K to induce desorption of the adsorbed molecules. During heating, the QMS monitored the desorbing species and any decomposition products. In all cases, adsorption and desorption of $(CF_3CF_2)_2O$, CF_3CH_2OH, and $C_{10}H_{22}$ were molecular and reversible with no indication of decomposition or reaction.

3. Results

3.1. CF_3CH_2OH, $(CF_3CF_2)_2O$, and $C_{10}H_{22}$ on a-CH_x Individually. Before studying the coadsorption of species, we have examined the adsorption of CF_3CH_2OH, $(CF_3CF_2)_2O$, and $C_{10}H_{22}$ individually on a-CH_x. CF_3CH_2OH was chosen to model the hydroxyl endgroups present in Fomblin Zdol. TPD spectra can be used to estimate the interaction strength of CF_3CH_2OH with a-CH_x films. Figure 1 shows TPD spectra of CF_3CH_2OH adsorbed at 100 K on the a-CH_{Quan} film. The spectra were generated

(13) Helmick, L. S.; Jones, W. R., Jr. *NASA Tech. Memor.* **1990**, 102−493.
(14) Perry, S. S.; Somorjai, G. A.; Mate, C. M.; White, R. *Tribol. Lett.* **1995**, *1*, 47−58.
(15) Cornaglia, L.; Gellman, A. J. *J. Vac. Sci. Technol., A* **1997**, *15*, 2755−2765.
(16) Meyers, J. M.; Gellman, A. J. *Surf. Sci.* **1997**, *372*, 171−178.
(17) Meyers, J. M.; Street, S. C.; Thompson, S.; Gellman, A. J. *Langmuir* **1996**, *12*, 1511−1519.
(18) Meyers, J. M.; Gellman, A. J. *Tribol. Lett.* **1996**, *2*, 47−55.
(19) Walczak, M. M.; Leavitt, P. K.; Thiel, P. A. *J. Am. Chem. Soc.* **1987**, *109*, 5621−5627.
(20) Walczak, M. M.; Thiel, P. A. *Surf. Sci.* **1989**, *224*, 425−450.
(21) Walczak, M. M.; Leavitt, P. K.; Thiel, P. A. *Tribol. Trans.* **1990**, *33*, 557−562.
(22) Paserba, K.; Shukla, N.; Gellman, A. J.; Gui, J.; Marchon, B. *Langmuir* **1999**, *15*, 1709−1715.

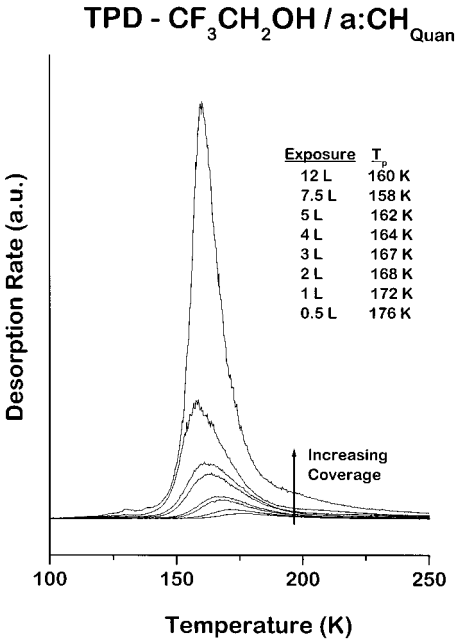

Figure 1. TPD spectra of CF_3CH_2OH on the a-CH_{Quan} surface obtained following various exposures at 100 K. The spectra were generated by monitoring mass 31 (CH_2OH^+). The heating rate was 2 K/s.

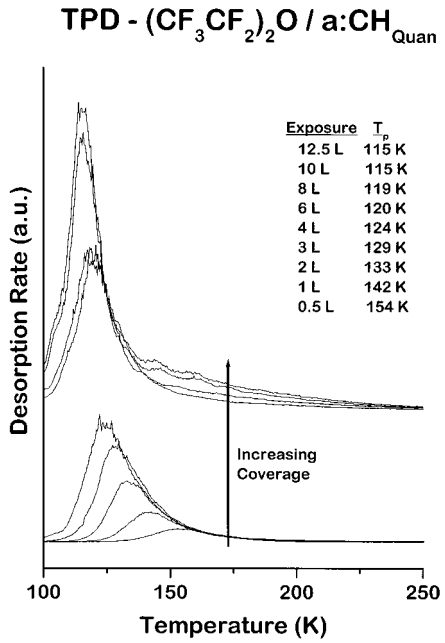

Figure 2. TPD spectra of $(CF_3CF_2)_2O$ on the a-CH_{Quan} surface obtained following various exposures at 100 K. The spectra were generated by monitoring mass 69 (CF_3^+). The heating rate was 2 K/s.

by using the QMS to monitor $m/q = 31$ (CH_2OH^+), the most intense ion in the fragmentation pattern of CF_3CH_2OH, as a function of temperature during heating at 2 K/s. One additional mass-to-charge ratio of $m/q = 69$ (CF_3^+) was monitored in order to detect the desorption of any decomposition products. No decomposition of CF_3CH_2OH was observed. At the lowest coverage, the adsorbed CF_3CH_2OH desorbs with a maximum rate at 176 K. As the exposure is increased, the desorption peak intensifies and shifts to lower temperatures until the monolayer is saturated. Following monolayer saturation, a desorption peak appears at 158 K that does not saturate with increasing coverage and displays zero-order kinetics indicative of bulk sublimation of multilayers. For the purposes of this work, the definition of one monolayer coverage is the lowest coverage at which zero-order desorption kinetics are observed. Zero-order desorption manifests itself as overlap in the initial desorption rates and alignment of the low-temperature leading edges of the desorption curves. The multilayer peak desorption temperature is consistent with values found for CF_3CH_2OH adsorbed on a-CH_x films (157 K),[23] a-CN_x films (159 K),[22] Cu(111) (165 K),[24] and ZrO_2 films (155 K).[25] The fundamental observation is that CF_3CH_2OH adsorbs reversibly on the a-CH_{Quan} film and desorbs with a peak desorption temperature that decreases with increasing coverage.

Perfluorodiethyl ether ($(CF_3CF_2)_2O$) was chosen as a model for the perfluoropolyalkyl ether backbone of Fomblin Zdol. Figure 2 shows TPD spectra of $(CF_3CF_2)_2O$ adsorbed at 100 K on the a-CH_{Quan} film. The spectra were generated by monitoring $m/q = 69$ (CF_3^+), as a function of temperature during heating at 2 K/s. Two additional mass-to-charge ratios of $m/q = 50$ (CF_2^+) and $m/q = 31$ (CF^+) were monitored in order to detect the desorption of any decomposition products. No decomposition of $(CF_3CF_2)_2O$ was observed. At the lowest coverage, the adsorbed $(CF_3CF_2)_2O$ desorbs with a maximum rate at 154 K. The multilayer peak desorption temperature is 115 K and is consistent with values found for $(CF_3CF_2)_2O$ adsorbed on a-CH_x (113 K),[15,23] a-CN_x films (118 K),[22] Al(110) (111 K),[16] Cu(111) (122 K),[17] and ZrO_2 (125 K).[25] As in the case of CF_3CH_2OH, the fundamental observation for $(CF_3CF_2)_2O$ is that adsorption is reversible on the a-CH_{Quan} film and the desorption peak temperature decreases with increasing coverage.

Decane ($C_{10}H_{22}$) adsorption onto the a-CH_x films was used to simulate the effects of hydrocarbon contamination. Figure 3 shows TPD spectra of $C_{10}H_{22}$ adsorbed at 100 K on the a-CH_{Quan} film. The spectra were generated by monitoring $m/q = 57$ ($C_4H_9^+$), as a function of temperature during heating at 2 K/s. At the lowest coverage, the adsorbed $C_{10}H_{22}$ desorbs with a maximum rate at 225 K. The multilayer peak desorption temperature is 188 K and is consistent with values found for $C_{10}H_{22}$ adsorbed on graphite (193 K)[26] and Pt(111) (196 K).[27] As in the cases of $(CF_3CF_2)_2O$ and CF_3CH_2OH, $C_{10}H_{22}$ adsorbs and desorbs reversibly without reaction on the a-CH_{Quan} film. One of the important points to observe is that since the desorption temperature range of the $C_{10}H_{22}$ is higher than those of either $(CF_3CF_2)_2O$ or CF_3CH_2OH its coverage is not changing during the desorption of $(CF_3CF_2)_2O$ and CF_3CH_2OH.

The exact conditions used for the preparation of a-CH_x films used in the data storage industry vary among manufacturers. The objective of our program to study the surface chemistry and properties of these films has been to identify the chemical characteristics that are common to all films and independent of their source. To that end, the experiments described above have also been performed on a-CH_x films provided by the Seagate Corp. The desorption spectra of $(CF_3CF_2)_2O$, CF_3CH_2OH, and $C_{10}H_{22}$ on the a-CH_{Quan} film shown in Figures 1, 2, and 3, respectively, are all qualitatively similar to those obtained

(23) Lei, R. Z.; Gellman, A. J. *Langmuir* **2000**, *16*, 6628−6635.
(24) McFadden, C. F.; Gellman, A. J. *Langmuir* **1995**, *11*, 273−280.
(25) Maurice, V.; Takeuchi, K.; Salmeron, M.; Somorjai, G. A. *Surf. Sci.* **1991**, *250*, 99−111.
(26) Paserba, K.; Gellman, A. In preparation.
(27) Sexton, B. A.; Hughes, A. E. *Surf. Sci.* **1984**, *140*, 227−248.

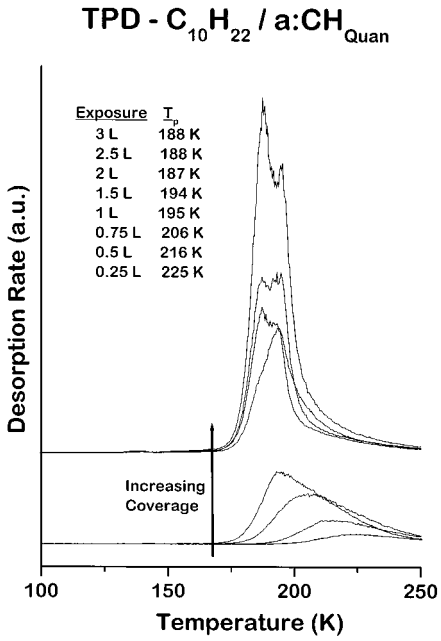

Figure 3. TPD spectra of $C_{10}H_{22}$ on the a-CH_{Quan} surface obtained following various exposures at 100 K. The spectra were generated by monitoring mass 57 ($C_4H_9^+$). The heating rate was 2 K/s.

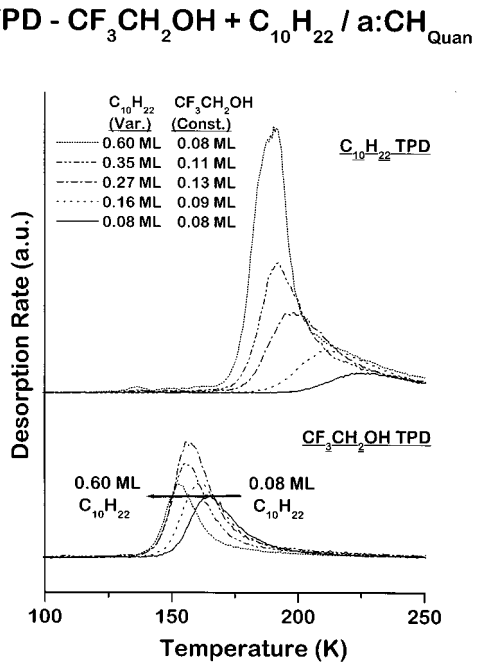

Figure 4. TPD spectra of coadsorbed CF_3CH_2OH and $C_{10}H_{22}$ on the a-CH_{Quan} surface obtained following adsorption at 100 K. Each pair of spectra illustrated with a given line type in the top and bottom halves of the figure corresponds to one experiment with a given coverage of $C_{10}H_{22}$ (variable from 0.08 to 0.60 ML) coadsorbed with CF_3CH_2OH (constant at 0.10 ± 0.02 ML). Examination of the CF_3CH_2OH TPD spectra reveals that the peak desorption temperature decreases with increasing $C_{10}H_{22}$ coverage. $C_{10}H_{22}$ was adsorbed onto the surface before the CF_3CH_2OH. The spectra were generated by simultaneously monitoring mass 31 (CH_2OH^+) and 57 ($C_4H_9^+$). The heating rate was 2 K/s.

on the a-CH_{Seag} films and on films obtained from other manufacturers and described in previous work.[15,22,28] All three molecules adsorb reversibly without reacting, and their desorption spectra reveal peaks that shift to lower temperatures with increasing coverage.

3.2. Coadsorption of $C_{10}H_{22}$ and CF_3CH_2OH on a-CH_x. Alkane hydrocarbon contamination effects on the interaction of Fomblin Zdol endgroups with a-CH_x films have been examined by studying the coadsorption of CF_3CH_2OH with increasing coverages of $C_{10}H_{22}$. Figure 4 shows the TPD spectra of coadsorbed CF_3CH_2OH and $C_{10}H_{22}$ on the a-CH_{Quan} overcoat. The order of adsorption onto the a-CH_{Quan} overcoat was $C_{10}H_{22}$ followed by CF_3CH_2OH, and both were exposed with the film held at or below 100 K. The CF_3CH_2OH coverage was kept constant at 0.10 ±0.02 ML, while the $C_{10}H_{22}$ coverage ranged from 0.08 to 0.60 ML. Due to the slow pumping characteristics of CF_3CH_2OH, it was difficult to reproducibly generate identical coverages. The spectra were generated by simultaneously monitoring mass 31 (CH_2OH^+) and 57 ($C_4H_9^+$) at a heating rate of 2 K/s. Several additional mass-to-charge ratios were monitored to verify that the only species observed in the desorption spectra were $C_{10}H_{22}$ and CF_3CH_2OH and there was no decomposition or reaction.

When looking at the spectra in Figure 4, it is important to remember that TPD measures the desorption rate at a given temperature. The peak desorption temperature is defined as the temperature at the maximum desorption rate. From the peak desorption temperature, one can estimate the desorption energy of the CF_3CH_2OH desorbing from the a-CH_x surface using Redhead's analysis method.[29] Examination of the CF_3CH_2OH TPD spectra shows that the CF_3CH_2OH peak desorption temperature systematically decreases with increasing $C_{10}H_{22}$ coverage. This indicates that the desorption energy of CF_3CH_2OH decreases with increasing $C_{10}H_{22}$ coverage.

Coadsorption of $C_{10}H_{22}$ and CF_3CH_2OH was also studied at other CF_3CH_2OH coverages greater than 0.10 ML. The results are found in Figure 5, which shows the CF_3CH_2OH desorption energy as a function of CF_3CH_2OH coverage with various constant coverages of coadsorbed $C_{10}H_{22}$. One can clearly see from Figure 5 that the desorption energy of CF_3CH_2OH decreases with increasing $C_{10}H_{22}$ coverage. Furthermore, a $C_{10}H_{22}$ coverage of 0.20 ML was sufficient to decrease the CF_3CH_2OH desorption energy to that of the multilayer.

In addition to experiments on the a-CH_{Quan} surface, experiments have been performed on an a-CH_{Seag} surface in order to determine the effects of overcoat source and composition on $C_{10}H_{22}$−CF_3CH_2OH interactions. The coadsorption TPD spectra obtained on a-CH_{Seag} films are all qualitatively similar to those obtained on the a-CH_{Quan} films. The observation that $C_{10}H_{22}$ decreases the desorption energy of CF_3CH_2OH holds true for all three types of films.

3.3. Coadsorption of $C_{10}H_{22}$ and $(CF_3CF_2)_2O$ on a-CH_x. The effect of alkane contamination on the interaction of the ether backbones of PFPE lubricants with a-CH_x films has been examined by studying the coadsorption of $(CF_3CF_2)_2O$ with $C_{10}H_{22}$. Figure 6 shows TPD spectra of $(CF_3CF_2)_2O$ and $C_{10}H_{22}$ coadsorbed on the a-CH_{Quan} surface. The order of exposure was $C_{10}H_{22}$ first followed by $(CF_3CF_2)_2O$ with the a-CH_{Quan} film held at 100 K. The $(CF_3CF_2)_2O$ coverage was kept constant at 0.10 ± 0.01 ML while the $C_{10}H_{22}$ coverage ranged from 0.00 to 0.18 ML. The spectra were generated by simultaneously monitoring $m/q = 69$ (CF_3^+) and 57 ($C_4H_9^+$) and using a heating rate of 2 K/s. Several additional mass-to-charge ratios were monitored to verify that there was no decomposition or reaction between $(CF_3CF_2)_2O$ and $C_{10}H_{22}$.

(28) Shukla, N.; Gellman, A. J.; Gui, J. *Langmuir* **2000**, *16*, 6562−6568.
(29) Redhead, P. A. *Vacuum* **1962**, *12*, 203−211.

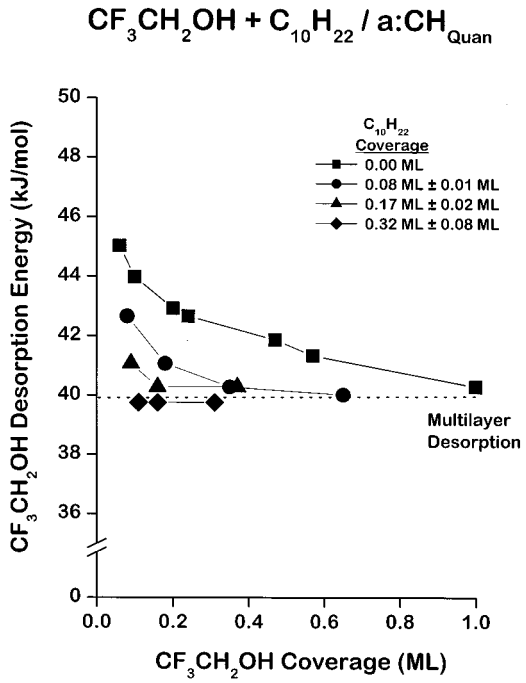

Figure 5. CF_3CH_2OH desorption energy as a function of CF_3CH_2OH coverage on the a-CH_{Quan} film at various constant coverages of coadsorbed $C_{10}H_{22}$. The desorption energies were obtained from the CF_3CH_2OH peak desorption temperature found from TPD experiments using coadsorbed CF_3CH_2OH and $C_{10}H_{22}$. The CF_3CH_2OH desorption energy decreases with increasing coverages of coadsorbed $C_{10}H_{22}$.

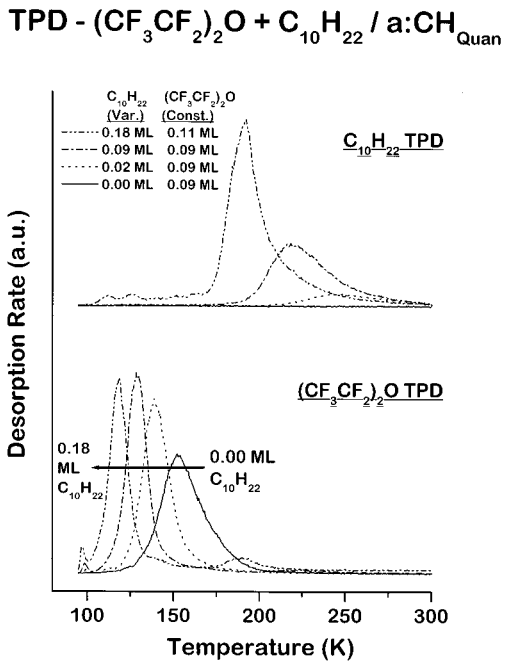

Figure 6. TPD spectra of coadsorbed $(CF_3CF_2)_2O$ and $C_{10}H_{22}$ on the a-CH_{Quan} surface obtained following adsorption at 100 K. Each pair of spectra illustrated with a given line type in the top and bottom halves of the figure corresponds to one experiment with a given coverage of $C_{10}H_{22}$ (variable from 0.00 to 0.18 ML) coadsorbed with $(CF_3CF_2)_2O$ (constant at 0.10 ± 0.01 ML). Examination of the $(CF_3CF_2)_2O$ TPD spectra reveals that the peak desorption temperature decreases with increasing $C_{10}H_{22}$ coverage. $C_{10}H_{22}$ was adsorbed onto the surface before the $(CF_3CF_2)_2O$. The spectra were generated by simultaneously monitoring mass 69 (CF_3^+) and 57 ($C_4H_9^+$). The heating rate was 2 K/s.

As in the case of CF_3CH_2OH coadsorption with $C_{10}H_{22}$, there was no evidence of any reaction between the $(CF_3CF_2)_2O$ and the $C_{10}H_{22}$.

Qualitatively, the TPD spectra of coadsorbed $(CF_3CF_2)_2O$ and $C_{10}H_{22}$ are identical to those of coadsorbed CF_3CH_2OH and $C_{10}H_{22}$. Figure 6 clearly shows a systemic decrease in the peak desorption temperature of $(CF_3CF_2)_2O$ as a result of increasing $C_{10}H_{22}$ coverage. Redhead analysis indicates that the desorption energy of $(CF_3CF_2)_2O$ decreases with increasing $C_{10}H_{22}$ coverage. Coadsorption experiments with higher coverages of $C_{10}H_{22}$ were conducted, and the results are captured in Figure 7. Figure 7 shows that the $(CF_3CF_2)_2O$ desorption energy decreases with increasing coverage at all coverages of coadsorbed $C_{10}H_{22}$. The $(CF_3CF_2)_2O$ desorption energy also decreases with increasing $C_{10}H_{22}$ coverage, and ~0.20 ML of $C_{10}H_{22}$ was sufficient to displace $(CF_3CF_2)_2O$ into the multilayer adsorption regime.

To investigate the differences between a-CH_x films obtained from different sources, TPD experiments with coadsorbed $(CF_3CF_2)_2O$ and $C_{10}H_{22}$ were performed on the a-CH_{Seag} films. Although there are subtle differences in the TPD spectra obtained on the a-CH_{Seag} and the a-CH_{Quan} films, the basic observation that coadsorbed $C_{10}H_{22}$ decreases the desorption energy of the $(CF_3CF_2)_2O$ was made on both surfaces.

3.4. Coadsorption with Different Exposure Orders. To understand coadsorption experiments involving two or more species, it is important to explore whether the order or sequence of adsorption affects the results. If the system is in equilibrium, then the order of exposure should not matter. In short, reversing the order of exposure in our experiments does not affect the basic observation that $C_{10}H_{22}$ decreases the desorption energies of both CF_3CH_2OH and $(CF_3CF_2)_2O$. Figure 8 shows TPD spectra of CF_3CH_2OH and $C_{10}H_{22}$ coadsorbed on the a-CH_{Quan} surface at 100 K with different orders of exposure. Equivalent coverage TPD spectra of CF_3CH_2OH and $C_{10}H_{22}$ adsorbed individually are also plotted for comparison. The $C_{10}H_{22}$ coverage was kept constant at 0.15 ± 0.01 ML, and the CF_3CH_2OH coverage was kept constant at 0.10 ± 0.01 ML. There are some differences between the desorption spectra of the CF_3CH_2OH obtained with different exposure sequences. However, for both exposure sequences, it is evident that the peak desorption temperature of CF_3CH_2OH is lowered by the presence of coadsorbed $C_{10}H_{22}$. This indicates that the desorption energy of CF_3CH_2OH decreases with $C_{10}H_{22}$ coverage irrespective of the order of exposure.

Coadsorption experiments in which the order of exposure to $(CF_3CF_2)_2O$ and $C_{10}H_{22}$ was reversed both reveal that coadsorbed $C_{10}H_{22}$ decreases the desorption energy of $(CF_3CF_2)_2O$. Figure 9 shows TPD spectra of coadsorbed $(CF_3CF_2)_2O$ and $C_{10}H_{22}$ with different orders of exposure and TPD spectra of $(CF_3CF_2)_2O$ and $C_{10}H_{22}$ adsorbed individually on the a-CH_{Quan} surface. The $C_{10}H_{22}$ coverage was kept constant at 0.12 ± 0.01 ML, and the $(CF_3CF_2)_2O$ coverage was kept constant at 0.22 ± 0.01 ML. As in the case of coadsorbed CF_3CH_2OH and $C_{10}H_{22}$, there are some subtle differences between the spectra obtained with different orders of exposure. However, it is clear that the $(CF_3CF_2)_2O$ peak desorption temperature was lowered by the presence of coadsorbed $C_{10}H_{22}$ irrespective of exposure sequence. Apparently, the desorption energies of both $(CF_3CF_2)_2O$ and CF_3CH_2OH decrease with $C_{10}H_{22}$ coverage irrespective of the order of exposure.

Although the primary focus of this work has been the effect of $C_{10}H_{22}$ contamination on the adsorption of CF_3CH_2OH and $(CF_3CF_2)_2O$, it is important to note that at the same time CF_3CH_2OH and $(CF_3CF_2)_2O$ also influence

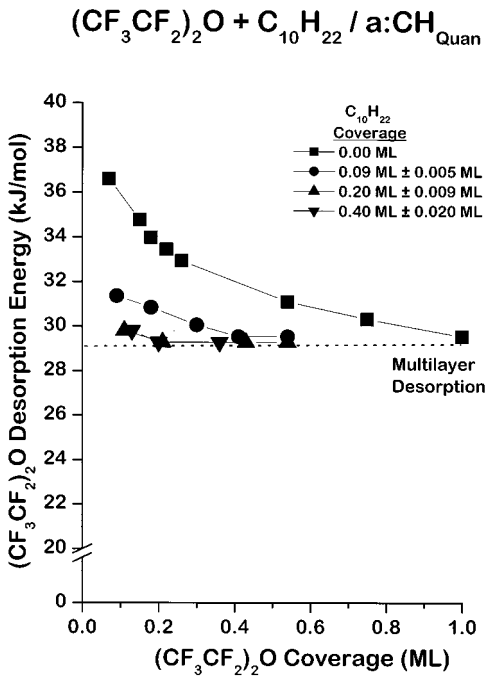

Figure 7. $(CF_3CF_2)_2O$ desorption energy as a function of $(CF_3CF_2)_2O$ coverage on the a-CH_{Quan} film at various constant coverages of coadsorbed $C_{10}H_{22}$. The desorption energies were obtained from the $(CF_3CF_2)_2O$ peak desorption temperature found from TPD experiments using coadsorbed $(CF_3CF_2)_2O$ and $C_{10}H_{22}$. The $(CF_3CF_2)_2O$ desorption energy decreases with increasing coadsorbed $C_{10}H_{22}$.

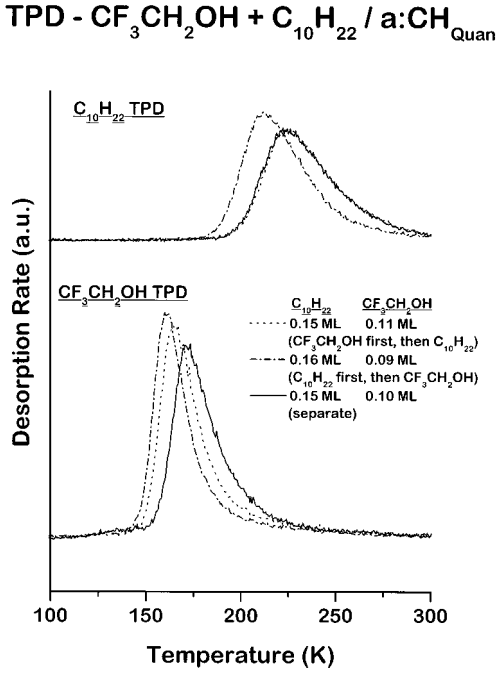

Figure 8. TPD spectra of coadsorbed CF_3CH_2OH and $C_{10}H_{22}$ with different orders of exposure and TPD spectra of CF_3CH_2OH and water adsorbed individually on an a-CH_{Quan} surface at 100 K. The presence of $C_{10}H_{22}$ decreases the peak desorption temperature of CF_3CH_2OH. The $C_{10}H_{22}$ coverage was kept constant at 0.15 ± 0.01 ML. The CF_3CH_2OH coverage was kept constant at 0.10 ± 0.01 ML. The spectra were generated by simultaneously monitoring mass 31 (CH_2OH^+) and 57 ($C_4H_9^+$). The heating rate was 2 K/s.

the desorption of $C_{10}H_{22}$. This effect can be observed from the $C_{10}H_{22}$ TPD spectra in Figures 8 and 9. The model lubricants tend to facilitate $C_{10}H_{22}$ desorption. This effect

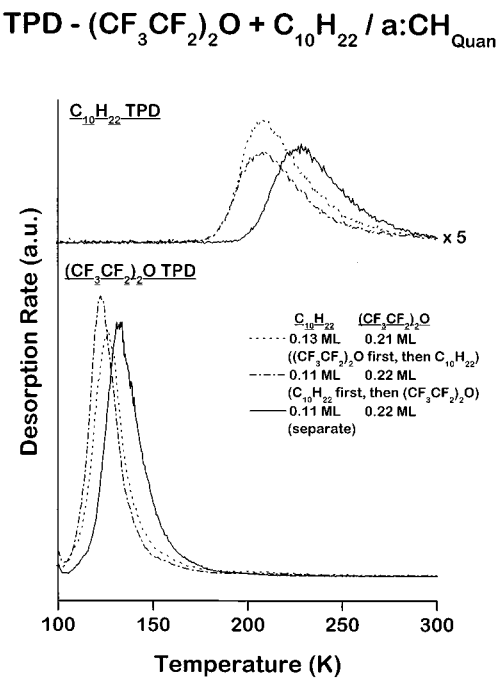

Figure 9. TPD spectra of coadsorbed $(CF_3CF_2)_2O$ and $C_{10}H_{22}$ with different orders of exposure and TPD spectra of $(CF_3CF_2)_2O$ and water adsorbed individually on an a-CH_{Quan} surface at 100 K. The presence of $C_{10}H_{22}$ decreases the peak desorption temperature of $(CF_3CF_2)_2O$. The $C_{10}H_{22}$ coverage was kept constant at 0.12 ± 0.01 ML. The $(CF_3CF_2)_2O$ coverage was kept constant at 0.22 ± 0.01 ML. The spectra were generated by simultaneously monitoring mass 69 (CF_3^+) and 57 ($C_4H_9^+$). The heating rate was 2 K/s.

is both odd and surprising since at the onset of $C_{10}H_{22}$ desorption most, if not all, of the model lubricants have already desorbed from the disk surface. Further investigation of this observation is planned.

4. Discussion

4.1. Interactions of CF_3CH_2OH, $(CF_3CF_2)_2O$, and $C_{10}H_{22}$ with a-CH_x. The nature of the interaction of alcohols with amorphous nitrogenated carbon films (a-CN_x) was investigated by Paserba et al.[22] and has also been investigated on a-CH_x films by Shukla et al.[28] These studies of alcohol adsorption on the a-CH_x and a-CN_x films showed that fluorination of the alcohols increased the desorption energy. The implication is that alcohols interact with the a-CH_x film through hydrogen bonding.[22,28] Previous studies of the interaction of ethers with the a-CH_x overcoats showed that fluorination of the ethers lowers their desorption energies. On this basis, it was proposed that their interaction with the a-CH_x films occurs through a dative bond, formed via electron donation from the oxygen lone pair electrons to the amorphous film.[15,22]

A good measure of the interaction strength of the ethers and alcohols with the a-CH_x overcoat is their desorption energy (E_d). The desorption energies can be estimated using the Redhead equation,[29]

$$\frac{E_d}{RT_p^2} = \frac{\nu}{\beta} \exp\left(-\frac{E_d}{RT_p}\right) \quad (1)$$

where β is the heating rate, R is the universal gas constant, ν is a pre-exponential factor, and T_p is the peak temperature from the TPD spectra. The simplest assumption used to estimate E_d is that desorption is a first-order process with a pre-exponential of $\nu = 10^{13}$ s^{-1}. Figures

5 and 7 show the desorption energies of CF_3CH_2OH and $(CF_3CF_2)_2O$ on the a-CH_x as a function of coverage (the data in solid squares is for CF_3CH_2OH and $(CF_3CF_2)_2O$ adsorption without coadsorbed $C_{10}H_{22}$). These results illustrate that the desorption energies decrease with coverage. Our understanding of this is that the a-CH_x film surfaces are heterogeneous in nature and expose a variety of adsorption sites with a range of affinities for CF_3CH_2OH and $(CF_3CF_2)_2O$ adsorption. Those sites with the highest affinity are occupied first or at low coverages, and sites of ever decreasing adsorption affinity are occupied sequentially as the coverage increases. The fact that the a-CH_x surfaces are heterogeneous is not surprising. In principle, a carbon atom can adopt three different electronic configurations: sp^3, sp^2, and sp^1. Graphite and diamond have pure sp^2 and sp^3 electronic configurations, respectively, and a-CH_x films have a mixture of both sp^2 and sp^3 bonded carbon atoms.[30] This dual nature of the electronic structure of the carbon in a-CH_x films is one source of its surface heterogeneity. At a finer level of detail, the carbon atoms can be coordinated in a number of different ways including CCH_3, C_2CH_2, CC(H)═C, partially oxidized structures such as C═O, COH, and C−O−C groups, and carbon dangling bonds. It is not surprising that these films contain a variety of sites for molecular adsorption having a range of affinities for the adsorption of CF_3CH_2OH and $(CF_3CF_2)_2O$.[15,31] It is the heterogeneity of the carbon films that is responsible for the coverage-dependent peak desorption temperatures and the breadth of the desorption features at monolayer coverages, both of which are due to coverage-dependent desorption energies.

A second potential source of coverage dependence in the desorption energy is the interaction between molecules on the surface as coverage increases. In the context of that model, the apparent decrease in the desorption energy with coverage would be interpreted in terms of a repulsive interaction between adsorbed molecules. However, this has been ruled out by experiments performed on the Cu(111) surface[15−17] and on graphite,[28] both of which reveal weak attractive interactions between adsorbed CF_3CH_2OH and between adsorbed $(CF_3CF_2)_2O$. As such, the coverage dependence of the desorption energy of these species on the a-CH_x films is attributed predominantly to the heterogeneity of the film surface.

4.2. Effect of $C_{10}H_{22}$ on CF_3CH_2OH and $(CF_3CF_2)_2O$ Bonding to a-CH_x. Finally, having discussed the nature of the interactions of CF_3CH_2OH, $(CF_3CF_2)_2O$, and $C_{10}H_{22}$ with a-CH_x films, the focus of this work has been to address the nature of their intramolecular interactions when coadsorbed on these films. There are many possible mechanisms of $C_{10}H_{22}$−lubricant interaction on an a-CH_x overcoat. First, $C_{10}H_{22}$ might react with the lubricant on the overcoat or $C_{10}H_{22}$ might react with the overcoat itself and thus modify its interaction with the lubricant. However, there was no evidence of reaction observed in any of the TPD experiments conducted in this work. As a second mechanism for interaction, $C_{10}H_{22}$ might displace lubricant from the adsorption sites on the overcoat for which it has the greatest affinity. If $C_{10}H_{22}$, CF_3CH_2OH, and $(CF_3CF_2)_2O$ were to compete for adsorption onto the same sites, $C_{10}H_{22}$ with greater desorption energy would displace CF_3CH_2OH and $(CF_3CF_2)_2O$ from those sites forcing them to adsorb on sites for which they have a lower binding affinity. As a third interaction mechanism, $C_{10}H_{22}$ and lubricant adsorbed on different sites might interact with each other through space. As mentioned, previous work on the very homogeneous Cu(111) and graphite surfaces has revealed that the natural interactions between adsorbed CF_3CH_2OH and between adsorbed $(CF_3CF_2)_2O$ are attractive. Due to the inert nature of $C_{10}H_{22}$, we believe the heteromolecular interactions between $C_{10}H_{22}$ and fluorinated lubricant species should be nothing more than attractive van der Waals attractions.

The desorption energies of CF_3CH_2OH and $(CF_3CF_2)_2O$ on a-CH_x decrease with increasing $C_{10}H_{22}$ coverage. This decrease in desorption energy can be quantified directly from the TPD spectra by applying the Redhead equation. Examination of Figures 5 and 7 illustrates the decrease in desorption energy of the model lubricants with increasing coverage of coadsorbed $C_{10}H_{22}$. Furthermore, the model lubricants were displaced to their multilayer regimes with relatively little $C_{10}H_{22}$ contamination. This behavior can be explained by the displacement mechanism proposed by Lei and Gellman to explain the effects of water adsorption on the bonding of CF_3CH_2OH and $(CF_3CF_2)_2O$ to a-CH_x surfaces.[23] Those studies of humidity effects on PFPE bonding to a-CH_x found that the presence of water displaces $(CF_3CF_2)_2O$ to lower affinity adsorption sites. The a-CH_x surface has a variety of binding sites with a range of affinities for the adsorption of CF_3CH_2OH, $(CF_3CF_2)_2O$, and $C_{10}H_{22}$. Decane with the highest desorption energies will preferentially adsorb to those binding sites with the highest affinity. As a result, CF_3CH_2OH and $(CF_3CF_2)_2O$ will be displaced by the presence of $C_{10}H_{22}$ to lower affinity sites, resulting in lower desorption energies. It is important to note that the $C_{10}H_{22}$ desorption energy from a-CH_x is a sum of van der Waals interactions from many methylene units, in contrast to a hydrogen bond of CF_3CH_2OH and a dative bond of $(CF_3CF_2)_2O$ which are quite localized. Hence, the displacement of model lubricants to lower energy sites may not be solely due to the competition for high-affinity sites. It may be due to the fact that each $C_{10}H_{22}$ occupies a series of adjacent sites on the a-CH_x surface and displaces the model lubricants to lower affinity sites. This steric nature of adsorbed $C_{10}H_{22}$ may explain the displacement of the model lubricants to their multilayer regime with low $C_{10}H_{22}$ coverage.

4.3. Implications for Fomblin Zdol Interaction with a-CH_x. On a conventional hard disk, the a-CH_x overcoat and a thin layer of Fomblin Zdol are the only protection for the magnetic layer against head−disk contacts. There are many studies indicating that alkane contamination can influence the integrity of the head−disk interface.[7−12,32] In this investigation, we have determined that increasing alkane contamination decreases the desorption energies of both CF_3CH_2OH and $(CF_3CF_2)_2O$, representative of the hydroxyl end groups and ether-like linkages of Fomblin Zdol, respectively. These results suggest that alkane contamination produced by outgassing of various disk drive components weakens the interaction of Fomblin Zdol with the a-CH_x overcoat. The result is an increase in Fomblin Zdol mobility across the disk surface. Lubricant mobility is desired for replenishment in areas of the disk surface that have been depleted of lubricant by head−disk contact. However, fully mobile lubricants may be easily spun off the disk platter, decreasing the reliability and durability of the hard disk.

(30) Robertson, J. *Adv. Phys.* **1986**, *35*, 317−374.
(31) Yanagisawa, M. In *Tribology and Mechanics of Magnetic Storage Systems*; STLE Special Publication SP-36; Society of Tribologists and Lubrication Engineers: Park Ridge, IL, 1994; Vol. 9, pp 25−32.
(32) Jesh, M. S.; Segar, P. R. In *ASME/STLE Tribology Conference*; Society of Tribologists and Lubrication Engineers: Toronto, Canada, 1998; Vol. 98-TC-5E-2, pp 1−7.

5. Conclusions

TPD experiments were performed using CF_3CH_2OH or $(CF_3CF_2)_2O$ coadsorbed with $C_{10}H_{22}$ on a-CH_x films in order to gain insight into the molecular interactions between hydrocarbon contaminants, Fomblin Zdol, and a-CH_x overcoats. The results show that $C_{10}H_{22}$ weakens the interaction of both CF_3CH_2OH and $(CF_3CF_2)_2O$ with the a-CH_x overcoat, indicative of a displacement of CF_3CH_2OH or $(CF_3CF_2)_2O$ to adsorption sites with lower adsorption affinity. Furthermore, low coverages of coadsorbed $C_{10}H_{22}$ were sufficient to displace the CF_3CH_2OH and $(CF_3CF_2)_2O$ into their multilayer adsorption regimes. The implications of these results are that Fomblin Zdol should have higher mobility on the a-CH_x surface in the presence of alkane hydrocarbon contamination.

Acknowledgment. This paper is based upon work supported by the National Science Foundation through the Data Storage Systems Center at Carnegie Mellon under Grant No. ECD-8907068. The government has certain rights to this material. In addition, the authors thank the Quantum Corporation and the Seagate Corporation for supplying the a-CH_x surfaces used in this work.

LA010413T